Simulations of ethylene-oxygen rotating detonation waves under different local equivalence ratio

Han Peng, Ralf Deiterding
Aerodynamics and Flight Mechanics Group, University of Southampton
Southampton, Hampshire, United Kingdom

1 Introduction

The highly efficient rotating detonation engine (RDE) has been considered as one of the viable replacements for current propulsion and power generation systems that employ constant pressure combustion [1]. The visualization of the internal flow field in RDEs experiments is challenging since the detonation wave travels in an RDE at high temperature, high pressure and high speed. Numerical simulations provide an approach to studying the complex flow in RDEs. Some premixed simulations were conducted using hydrogen and hydrocarbon fuel [2, 3]. Yet, in realistic experimental tests, the premixed propellants may cause a backfire into the plenum if no specialized injectors are employed. It is hence necessary to conduct some simulations based on non-premixed injection [4].

To simulate the non-premixed injection, the injectors for fuel and oxidizer have been individually simulated in first 3-D simulations [5–7]. However, the extreme thermodynamic conditions in an RDE make 3-D simulations costly and challenging. The 2-D unwrapped plane is a simplified model to simulate the rotating detonation waves under the assumption that parameters are constant in the radial direction. The 2-D model has been extensively used in simulations of RDEs as it decreases the computational costs without missing the main features of the flow field [8, 9].

Another effective approach for simulating detonation problems is adaptive mesh refinement (AMR). The grids are refined dynamically in the regions where the physical variables change dramatically [10]. In the present work, the 2-D unwrapped plane of an annular RDE is simulated with adaptive meshes. Premixed ethylene/oxygen mixtures are injected through discrete slots under different prescribed equivalence ratios. The effects of the non-uniform local equivalence ratio on rotating detonation waves are studied.

2 Methodology

2.1 Numerical methods

Simulations in this work are based on the open-source mesh adaptation framework AMROC (Adaptive Mesh Refinement in Object-oriented C++) [11]. AMROC has been used previously for simulating

Correspondence to: h.peng@soton.ac.uk

detonation problems [12]. Here, we apply the AMROC-Clawpack finite volume module and the multi-component 2-D compressible Euler equations with a detailed chemical model are solved as governing equations. The inviscid flux is evaluated by a hybrid Roe/HLL scheme, cf. [11]. A second-order accurate MUSCL-Hancock scheme with Minmod limiter is used for the reconstruction. Strang splitting is adopted for the reactive source term and a simplified ethylene/oxygen reaction mechanism [13] is employed.

2.2 Numerical configurations

The computational domain of the 2-D unwrapped RDE is shown in Figure 1, which is a two-dimensional rectangular chamber with a length of 236 mm and a height of 50 mm referring to an actual micro RDE laboratory experiment [14]. The initial pressure in the whole domain is set to 0.1 MPa and the temperature is 300 K. Then a small region of [0, 10 mm] × [10mm, 20 mm] extent is initialized by setting the pressure to 1.5 MPa and the temperature to 2500 K in order to ignite the detonation directly. A triangular region, filled with stoichiometric ethylene/oxygen mixture, is used to sustain the propagation of the detonation in the first cycle. Otherwise, the chamber is filled with pure air to avoid that the high-temperature burned gas induces detonation in the reverse direction, which may occur in realistic ignition but is not being considered in present work.

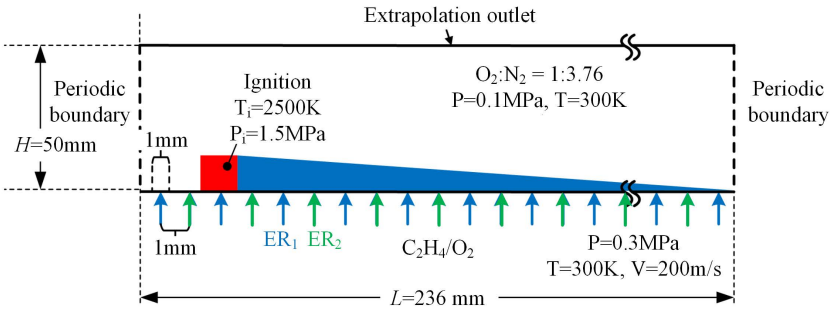

Figure 1: 2-D computational domain of the ethylene/oxygen RDE simulations.

The left and right sides are periodic boundaries to simulate the detonation propagation in a 3-D annular chamber. The top side is set as supersonic outflow boundary condition, where the physical variables are extrapolated from the inner domain. The premixed ethylene/oxygen mixtures are injected from 1 mm wide slots on the bottom that are spaced 1 mm apart. The axial velocity, static pressure and temperature of the inflow are prescribed in the ghost cells as shown in Figure 1. For each case, the equivalence ratio (ER) of adjacent slots is indicated by ER_1 and ER_2, respectively. Table 1 shows the difference between ER_1 and ER_2 ranging from 0 to 1 in six cases. As the mixtures are injected at the same velocity, the volumetric flow rate is constant. Hence, the global equivalence ratio is uniform in the different cases.

Table 1: Local equivalence ratio arrangements in the investigated cases.

Case	ER_1	ER_2	ER difference
1	1.0	1.0	0
2	0.9	1.1	0.2
3	0.8	1.2	0.4
4	0.7	1.3	0.6
5	0.6	1.4	0.8
6	0.5	1.5	1.0

All RDE cases in the present work use the following adaptive refinement parameters: Refinement flags are always set and the grid hierarchy is recomposed in every time step, namely the value of regridding is set as 1. The buffer width is 2 in order to mark two additional cells around each flagged cell. The prescribed threshold for the clustering algorithm is set to 0.7, which means that the procedure generates successively smaller grids until the ratio between flagged and all cells in every new grid is above the given threshold. The scalar gradients of density and pressure are computed as the refinement criteria. For the base mesh, there are 472 cells in the circumferential direction and 100 cells in the axial direction. Three types of grids are tested to simulate the 1-D stand-off detonation wave at 0.1 MPa and 300K. The refinement factor is 2 for each level. The minimum mesh size is 62.5 µm, 31.25 µm and 15.625 µm with 3, 4 and 5 refinement levels respectively.

As shown in Figure 2, the detonation wave is located virtually at the same position when the mesh is refined. The temperature profiles are also convergent. Although a higher pressure peak can be obtained by increasing the mesh refinement level up to 5, the four-level refinement is considered as a good trade-off between the computational accuracy and cost. The following 2-D calculations were performed on the high-performance computing cluster Iridis 5 at the University of Southampton, where 120 cores (Intel Xeon E5-2670 2.0 GHz) were used for each case. The total number of four-level cells is changed dynamically from 1.6 to 2.4 million. Typical run times for the RDE operating time 0.1 ms were approximately 7 to 8 days wall-clock time.

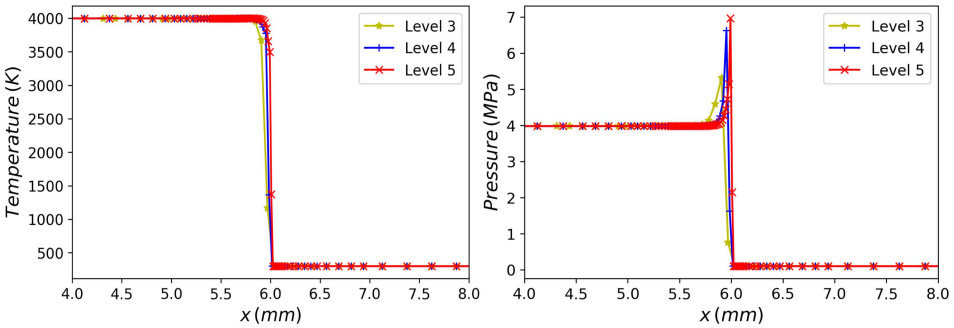

Figure 2: Temperature and pressure profiles of 1-D ethylene/oxygen detonation front.

3 Result

Figure 3 shows the instantaneous local equivalence ratio distribution in different cases with fully developed detonation waves. In Case 1, the stoichiometric mixtures are injected, and the local equivalence ratio is uniform in the mixture layer ahead of the detonation wave. In other cases, the differences of mixture mole fraction resulted in non-uniform local equivalence ratios. The premixed mixtures are injected vertically from the bottom. As a result, the propellants are not mixed adequately before being consumed. It is noted that only in Case 4 a four-wave mode is observed. In this case, the height of the fresh mixture layer is lower than for the other cases.

The temperature and temperature gradient distribution are shown in Figure 4. The multiple detonation waves are each followed by an oblique shock wave. Some weak compression waves are observed behind the detonation wave since the premixed gases are injected discretely. Each premixed jet is surrounded by a small amount of burned gas. In addition, the temperature gradient is large on the contact surface ahead of the detonation waves, where the premixed reactants are also consumed by the burned products.

Some probes have also been placed to monitor the pressure variations in the chamber. Figure 5 shows the pressure history of these probes in different cases from 0.6 ms to 0.9 ms simulated time. The numbers

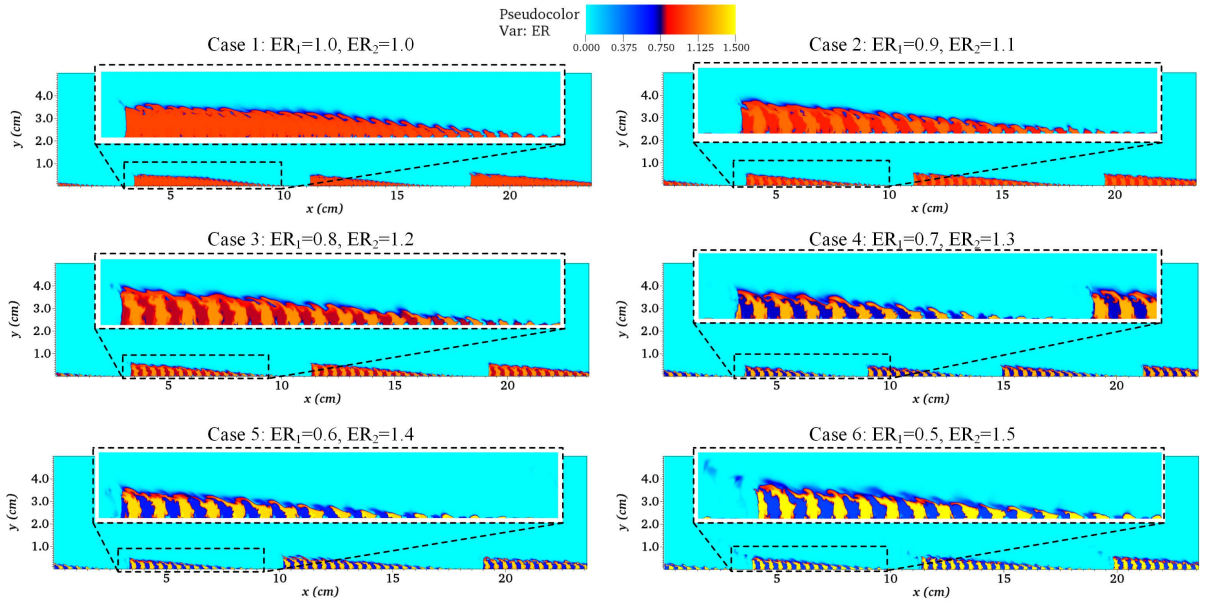

Figure 3: Pseudo-color images of local equivalence ratio (ER) under different injections.

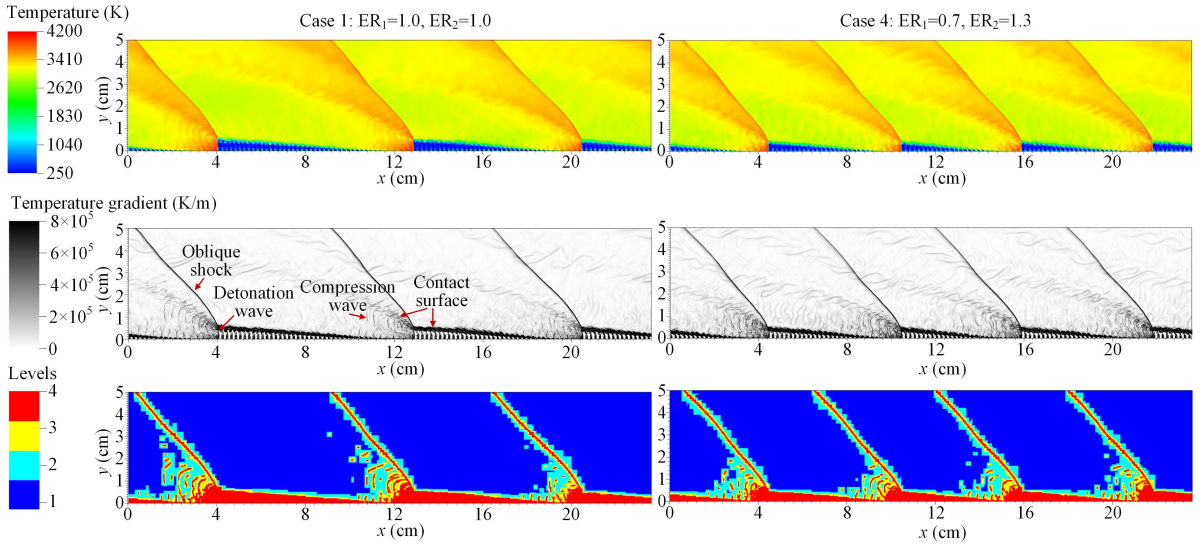

Figure 4: Pseudo-color images of temperature, temperature gradient and refinement level distribution under different injections.

in the figure legend indicate the circumferential coordinates of the probe locations. The height of the detonation wave is estimated from Figure 3, which ranges from 4.2 mm to 5.8 mm. Hence, these probes, which are 2 mm from the bottom wall, are able to measure the pressure of the detonation wave. From the pressure profiles, 11 or 12 strong pressure peaks are observed in Case 4, and 9 pressure peaks are observed in other cases, which corresponds to the number of waves as shown in Figure 4.

The flow velocity in the horizontal direction is computed by calculating the distance and time that the detonation wave requires to cross the probe. The average flow velocity can also be computed by calculating the interval of the cycle from the frequency of the pressure history. The average detonation velocity is computed through the horizontal flow and vertical injection velocity, considering the inclination of the detonation wave. As depicted in Figure 6, the average propagation velocity of detonation

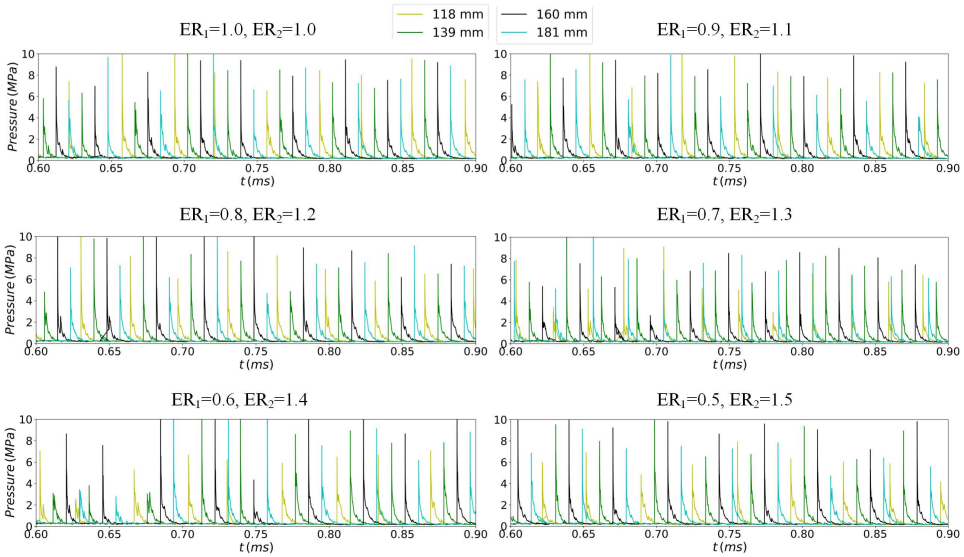

Figure 5: Pressure history from 0.6 ms to 0.9 ms.

waves declines when the local equivalence ratio increases. For all the cases, the detonation velocity is lower than the C-J velocity of a stochiometric mixture. The detonation velocity of the four-wave mode is lower than the velocity in other three-wave cases, even when the ER difference is large.

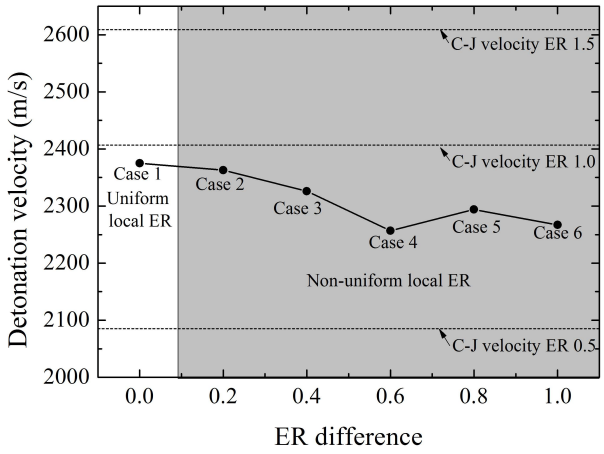

Figure 6: Average detonation velocity computed from the pressure profiles from 0.6 ms to 0.9 ms.

4 Conclusion

The effects of a non-uniform local equivalence ratio on rotating detonation waves are studied by numerical simulations on adaptive meshes. Premixed ethylene/oxygen mixtures are injected individually with a uniform global equivalence ratio. Stable multiple-wave modes are reproduced by the simulations. The results show that the number of detonation waves changes at a specific local equivalence ratio. Detonation velocity deficits are also observed when increasing the local equivalence ratio difference.

Acknowledgement

H. Peng acknowledges financial support from China Scholarship Council (CSC). The authors also acknowledge the use of the IRIDIS High Performance Computing Facility, and associated support services at the University of Southampton.

References

[1] Wolański P. (2013). Detonative propulsion. Proc. Combust. Inst. 34: 125-158.

[2] Zhou R, Wang JP. (2012). Numerical investigation of flow particle paths and thermodynamic performance of continuously rotating detonation engines. Combust. Flame 159: 3632–3645.

[3] Schwer D, Kailasanath K. (2013). Fluid dynamics of rotating detonation engines with hydrogen and hydrocarbon fuels. Proc. Combust. Inst. 34: 1991–1998.

[4] Lu FK, Braun EM. (2014). Rotating detonation wave propulsion: experimental challenges, modeling, and engine concepts. J. Propuls. Power 30: 1125–1142.

[5] Schwer D, Kailasanath K. (2015). Towards non-premixed injection modeling of rotating detonation engines. 51st AIAA/SAE/ASEE Joint Propulsion Conference No: 3782.

[6] Cocks PA, Holley AT, Rankin BA. (2016). High fidelity simulations of a non-premixed rotating detonation engine. 54th AIAA Aerospace Sciences Meeting No: 0125.

[7] Sun J, Zhou J, Liu SJ, Lin ZY. (2018). Numerical investigation of a rotating detonation engine under premixed/non-premixed conditions. Acta Astronaut. 152: 630–638.

[8] Fujii J, Kumazawa Y, Matsuo A, Nakagami S, Matsuoka K, Kasahara J. (2017). Numerical investigation on detonation velocity in rotating detonation engine chamber. Proc. Combust. Inst. 36: 2665-2672.

[9] Raj P, Meadows JW. (2020). Influence of Fuel Inhomogeneity and Stratification Length Scales on Rotating Detonation Combustor (RDC) Performance. AIAA Propulsion and Energy 2020 Forum No: 3875.

[10] Berger MJ, Colella P. (1989). Local adaptive mesh refinement for shock hydrodynamics. J. Comput. Phys. 82: 64-84.

[11] Deiterding R. (2003). Parallel adaptive simulation of multi-dimensional detonation structures. Dissertation.

[12] Peng H, Huang Y, Deiterding R, Luan ZY, Xing F, You YC. (2018). Effects of jet in crossflow on flame acceleration and deflagration to detonation transition in methane–oxygen mixture. Combust. Flame 198: 69-80.

[13] Singh DJ, Jachimowski CJ. (1994). Quasiglobal reaction model for ethylene combustion. AIAA J. 32: 213-216.

[14] Law H, Baxter T, Ryan CN, Deiterding R. (2021). Design and testing of a small-scale laboratory rotating detonation engine running on ethylene-oxygen. AIAA Propulsion and Energy 2021 Forum No: 3658.